International Journal of Computer Information Systems and Industrial Management Applications
ISSN 2150-7988 Volume 18(4s) 2026 pp. 925-945
https://doi.org/10.70917/ijcisim-2026-2608

Article

Integration of Computer Vision with Deep Feature Representation Learning for Robust Wheat Seed Variety Identification and Purity Analysis

B. Deepika[1], N. Shanmugapriya[2], R. Gopi[3]*

[1]Department of Computer Science & Engineering, Dhanalakshmi Srinivasan University, Tiruchirappalli (Trichy) – 621112, Tamil Nadu, India.
Email: deepi.b1992@gmail.com
[2]Department of Artificial Intelligence and Data Science, Dhanalakshmi Srinivasan University, Samayapuram, Tiruchirappalli (Trichy), Tamil Nadu, India.
Email: shanmugapriyan.set@dsuniversity.ac.in
[3]Department of Computer Science & Engineering, Dhanalakshmi Srinivasan Engineering College, Perambalur – 621212, Tamil Nadu, India.
Email: gopircse@gmail.com
Corresponding Author: N. Shanmugapriya, shanmugapriyan.set@dsuniversity.ac.in

Abstract: Wheat is the primary staple grain in temperate climates and is increasingly sought after in countries experiencing growth in their cities and industries. It is a primary food source that provides essential energy, protein, and other nutrients, and its rising demand is driven by factors like population growth and changing dietary habits. Identifying and classifying seed varieties is even conducted physically over direct visual assessment, which is time-consuming, labour-intensive, and prone to error. Thus, it is vital to develop a sophisticated, automated method that is economical and rapid to improve agricultural manufacture and grain integrity. To attain this goal, computer vision and artificial intelligence techniques have attained higher precision in detecting and classifying the complex seed features. Since the advent of convolutional neural networks (CNNs), several studies have focused on applying deep learning methods in the domain of agricultural. Deep learning is an advanced model for image processing and data analysis. Therefore, this study introduces an Automated Wheat Seed Variety Classification and Purity Assessment using the Optimal Deep Learning (AWSVCPA-ODL) technique. The purpose of the AWSVCPA-ODL technique is to accurately analyse wheat seed images using computer vision and deep learning, enabling robust varietal identification and reliable purity assessment. At the initial stage, the proposed AWSVCPA-ODL technique follows two pre-processing steps: Gaussian filtering-based noise elimination and contrast enhancement to improve the quality of input images for further analysis. For feature extraction, the AWSVCPA-ODL technique employs a feature fusion process that combines EfficientNet, SqueezeNet, and a Capsule network. A bidirectional gated recurrent unit with self-attention is applied for the detection and classification of wheat variety and its purity. To further enhance the performance of classification model, the Adabelief hyperparameter optimizer is applied. To ensure the better performance of proposed AWSVCPA-ODL method, a wide range of simulations were performed on the benchmark database. The results indicated that the proposed technique outperformed existing models.
Keywords: Wheat Seeds; Purity Analysis; Feature Fusion; Deep Learning; Parameter Optimization

1. Introduction

Wheat is a main food crop global. Different types of food offer a wide range of the world's nutrients equated with those from diverse cereal grains [1]. Wheat delivers the world's eatable dry grains, accounting for approximately 28 to 60 per cent of daily calories in emerging countries. Food consumption is predictable to be double by 2050, along with the rising demand for higher-quality nutrition for healthy nutrition [2]. Furthermore, growing grain yield with corresponding unit area to maintain the final user-value persists as a worldwide nutritional issue. The nutritional and composition quality of wheat grain have a major effect on human health and wellness [3]. Hence, conditions impacting not only wheat yield but also wheat quality need greater focus. Recognizing the various types of wheat seed is not only choose appropriate seeds but also about protecting the preferences of business and agriculturists. Accordingly, it is required to identify different forms of wheat seeds to control wheat seed market and production non-destructively and quickly [4].

The nutritional and quality attributes of flour are exactly connected with the content and categories of fatty acids and starch in wheat. It is prominent that the softness of baked products and the stability in noodles food is affected by the complex ingredients of the flour [5]. The biological technique is generally employed to differentiate the wheat variations because various seed types have variety of components which influence the quality of flour and wheat. Seed quality identifies the quality of the ultimate agricultural products, cost, and production rate [6]. Quality control specialists take samples from the seeds formed after analysis, and the seeds and the plants are manually approved in seed laboratories of various research organisations in the counties [7]. A decision for grading wheat is insufficient to the analysis of the visual qualities of seed sample measurement s by trained persons. Manual performances impact the analyzed outcomes under the subjective experiences of the researcher [8]. Human errors and mind fluctuations lead to difficulties in quality control analysis of wheat seeds. It is a complex, time-consuming task that needs a skilled person. Wheat production research workers commonly face these difficulties during manual measurement and comparison of the wheat seed's visual qualities [9].

Current research has demonstrated that image processing is a major component in the development of automatic evaluation systems for crops. Machine learning (ML) is a particularly important domain of artificial intelligence (AI), which involves computer systems capable of evaluating data and improving comprehension without human involvement. Specific methods support these systems by examining data and transforming them into an insightful experience [10]. Various researches are performed to analyse agricultural data to develop yield. It is employed to make geographic clusters based on the soil's fertility for different types of crops or determine a connection between rainfall intensity and agricultural productivity [11]. Many research activities have examined the implementation of numerous techniques by labelling agricultural data with the help of classification methods under historical samples. The nonlinear pattern of model parameters is measured, and future tendencies are anticipated by applying ML and deep learning (DL) methods, namely Generative Adversarial Network (GAN), Recurrent Neural Network (RNN), and Convolutional Neural Network (CNN) [12].

To overcome the challenges of visual variability, inter-varietal similarity, and unreliable purity estimation in wheat seed analysis, this paper introduces an Automated Wheat Seed Variety Classification and Purity Assessment using Optimal Deep Learning (AWSVCPA-ODL) system. The proposed AWSVCPA-ODL model aims to accurately detect and assess the seed variety and its purity using advanced deep learning techniques. The proposed model incorporates image preprocessing, multi-model feature fusion, a deep learning-based classifier, and optimization to ensure precise varietal detection and effective purity classification. The key contributions of this article are as follows:

- Present a multi-model feature fusion tactic, which combines EfficientNet, SqueezeNet, and Capsule network (CapsNet), allowing the representation of hierarchical, structural features vital for classifying wheat varieties and purity assessment.
- Design a self-attention bidirectional gated recurrent unit (SA-BiGRU) classifier, which efficiently learns long-term relations and emphasizes the most discriminative seed features, thus allowing precise wheat variety and purity classification.
- Utilize the AdaBelief optimizer for hyperparameter tuning, which helps attain better convergence, generalization capability, and better classification results.
- Implement comprehensive simulation experiments using benchmark datasets and evaluate that the proposed AWSVCPA-ODL model performed better compared to other models across various evaluation metrics, demonstrating its efficiency for real-world agricultural quality analysis.

2. Prior Studies on Wheat Seed Analysis

In this part, an overview of existing studies on the wheat seed analysis is discussed. In [13], presented an optical recognition method for wheat seed purity was presented that depends on sample contrastive as well as generation learning approach. This model initially used a linear generation approach for expanding an impurity sample, therefore improving the variety of impurity examples and enhancing the imbalance among the negative as well as positive examples. Then, the contrastive learning loss function is proposed for training the optical recognition technique that depends on the DCNN, also for improving the feature variations among the negative and positive samples, and for enhancing the model's detection precision for unknown impurity examples. Gu et al. [14] proposed a quick and precise identification approach for wheat seed with differing attentions of SLs, using two-view hyperspectral information fusion integrated with DL models. Wheat seeds are taken in various SLs attentions, & hyperspectral information is gathered from either the endosperm or embryo surface. For efficiently leveraging the spectral information from Concat, Stack, Parallel, and both sides of the seeds, data fusion approaches are used. Janapati et al. [15] introduced the growth of an enabled device for actual wheat seeds quality classification. With the utilization of actual camera technology as well as DL models such as YOLO, it provides rapid, non-destructive examination of significant seed quality metrics. To ensure the precision and reliability of seed quality recognition, the solution focuses on the method structure, camera combination, and YOLO.

Moreover, to enhance seed quality control, the combination of DL and IoT provides a framework for an agricultural procedure optimiser that increases crop yields and reduces resource waste.

Guo et al. [16] presented a lightweight wheat seed detection method named LWheatNet. The technique combines a mixed-attention mechanism with manifold stacked inverted residual network. Initially, propose a mixed-attention module that integrates spatial and channel attention separately. The method improves feature extraction in wheat seed imaging. Furthermore, stacked inverted residual convolutional networks for feature extraction from wheat seed imagery. Every network contains 3 key layers, each including multiple basic units and one downsampling unit. Xing et al. [17] developed a CNN-based image-detection approach for wheat seeds, namely GC_DRNet. This technique depends on the ResNet-18 model and integrates the dense network concept with a global contextual module, changing the residual mechanism to a dense residual mechanism, decreasing the system model's measures, and enhancing the network's detection precision. The development of the wheat sector and the defense of breeding rights may advance the precise classification of wheat varieties. In [18], presented an innovative hybrid CNN united with a hyperspectral image is employed for wheat seeds classification. Hyperspectral images provide spectral-spatial data concurrently, offering a set of external and internal features for each example. For taking full benefit of the spatia-spectral data, the hyperspectral imaging of wheat seed was examined by mixture convolution. Primarily, average spectra are obtained and processed into 1D convolutions for spectral feature extraction.

Jin et al. [19] proposed a spatial and spectral feature extractor model for identifying seeds. Then, PCA is used to excerpt features from the spatial-spectral information. Eventually, the SVM optimizes and trains the method. Though most existing hyperspectral identification approaches use only spectral data and ignore spatial data, this leads to unsatisfactory identification results. Barysheva et al. [20] proposed a NN research of the information on wheat seeds quality. The examination of bioelectrical signs of wheat seed that depend on NN may be utilized in practice for the solution of double issues, such as the assessemnt of cleaning line quality and diagnostics of seed material quality. This article presents outcomes of early data preparation and NN formation and examines the training information for dual practical identification issues. A literature survey of techniques for wheat seed quality and variety analysis is presented in Table 1.

Table 1 Comparative review of previous research

Reference	Methodologies	Datasets	Findings	Research aim
Yan et al. [13]	DCNN and SVM models.	Image dataset.	Accuracy of 95.33 %.	Develop an optical seed-purity model handling imbalanced data and unknown impurities using contrastive learning.
Gu et al. [14]	SCNN, AdaBoost, and GBDT models.	Hyperspectral dataset.	Accuracy of 99.26 %.	Establish a dual-view hyperspectral deep-learning approach for rapid detection of wheat seed strigolactones.
Janapati et al. [15]	DL models	NA	Accuracy of 93.10 %.	Formulate an IoT-enabled DL system for real-time, non-destructive detection of wheat seed quality.
Guo et al. [16]	CNN method	Image dataset.	Accuracy of 98.59 %.	The model is designed to achieve accurate, efficient real-time classification of

				wheat seed varieties.
Xing et al. [17]	DL algorithm	CIFAR-100 dataset.	Accuracy of 96.98 %.	Enhanced a lightweight DL model to achieve accurate and efficient identification of wheat seed varieties
Zhao et al. [18]	CNN approach	Hyperspectral dataset.	Accuracy of 95.65 %.	A hybrid hyperspectral feature-extraction model to rapidly and accurately assess wheat seed purity.
Jin et al. [19]	PCA and SVM techniques.	Hyperspectral dataset.	Accuracy of 97.64 %.	Create a spatial-spectral feature extraction approach to rapidly and accurately classify wheat seeds.
Barysheva et al. [20]	Neutral- Network model	NA	Achieved better performance.	Investigate neural network-based analysis of wheat seed bioelectrical signals to assess quality and perform classification.

3. Methodological Pipeline

The proposed AWSVCPA-ODL model follows a systematic pipeline for automated wheat seed variety classification and purity assessment, encompassing robust preprocessing, feature fusion strategy, classification, and optimization. Fig. 1 depicts the complete architectural design of the AWSVCPA-ODL technique. The overall workflow of the proposed model comprises numerous stages demonstrated in Fig. 1. First, a two-step preprocessing step is implemented, where GF is utilised for noise removal and contrast enhancement technique to boost image quality and structural visibility of seed patterns. After preprocessing, a feature extraction process is performed through the fusion of EfficientNet, SqueezeNet, and CapsNet for capturing complementary spatial and hierarchical attributes of wheat seed images. Following this, the captured features are fed into the SA-BiGRU-based classification mechanism, which efficiently models temporal relationships among the fused representations while highlighting the most informative patterns for variety detection and purity classification. To further enhance the classification outcomes, the AdaBelief optimizer is leveraged for stable convergence and enhanced generalization capability.

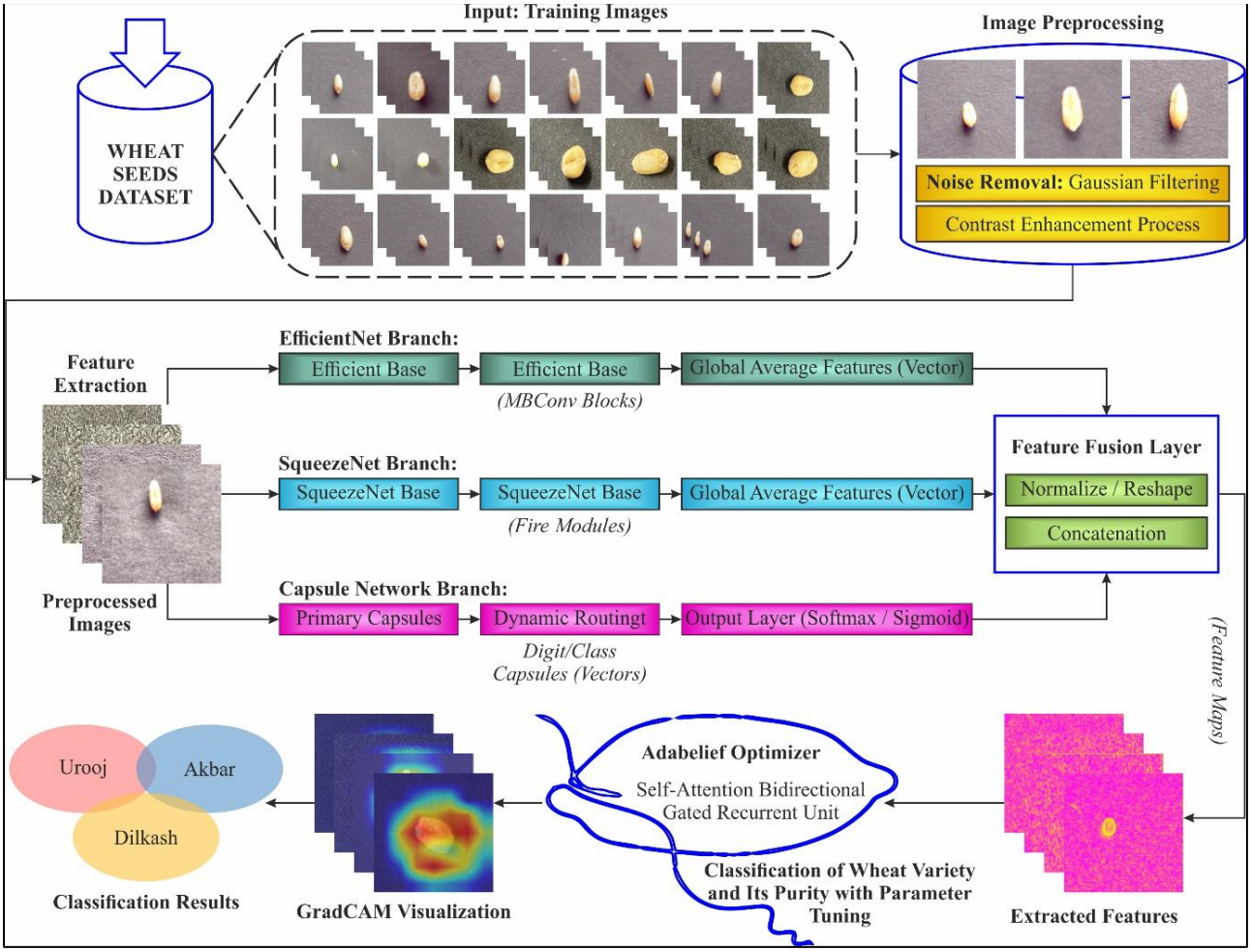

Fig. 1. Complete architectural design of the AWSVCPA-ODL technique

3.1. Input Preprocessing Module

In the preprocessing step, the proposed model prepares the input images as follows. GF is applied to remove noise and enhance contrast, thereby improving the seed image quality for subsequent analysis. GF is widely employed in image smoothing. The GF does not weight every value in the neighbourhood equally, unlike the mean filter. GF neighborhood size is calculated to employ σ and Standard Deviation. GF is usually selected owing to its non-sharp transition and distance-dependent weight. For the kernel value at pixel r rows and c columns, the mathematical formualtion is given below:

$$k_{r,c} = \frac{1}{2\pi\sigma^2}\, exp\left(-\frac{r^2 + c^2}{2\sigma^2}\right) \tag{1}$$

GF is are shortened at about 4σ, and this value is fairly nearer to 0.

After noise reduction, the presented model leverages a dedicated contrast improvement process to increase the visual clarity of wheat seed images. Because a variety of seed are frequently revealing subtle variations in texture, color intensity and surface patterns, raw images can endure from lower contrast, uneven illumination, or poor visual separation among seed regions [21]. To tackle these issues, the presented approach employs an adaptive contrast improvement method that reallocates pixel intensities to emphasise fine-grained discriminative attributes. To stretch the dynamic array of image histogram and increasing local variations, the procedure improves edge visibility, surface contours, and morphological features are vital for precise variety identification. This enhancement not only enhances the proficiency of feature extraction in the succeeding deep representation learning module but also substantially improves the reliability and robustness of the entire varietal recognition and purity evaluation pipeline.

3.2. Fusion-Based Feature Extraction

For feature extraction, the fusion of three architectures, integrating EfficientNet, SqueezeNet, and CapsNet, which extracts the most crucial features contributing to seed variety classification.

3.2.1. EfficientNet

EfficientNet has developed the most promising architectures in image classification. They proposed an innovative method for scaling CNNs, attaining advanced precision with fewer parameters and decreased computation expense. The structure depends on a compound scaling approach, which uniformly scales each dimension of the network, width, depth, and resolution, utilizing a collection of carefully selected coefficients of scaling. This model contains various methods, varying from EfficientNet-BO to EfficientNet-B7, each variant in size and difficulty [22]. The base technique, EfficientNet-B0, is very important for its balance between efficiency and performance. It uses the Mobile Inverted Bottleneck Convolution (MBConv) layers, integrated with the squeeze-and-excitation optimizer, to improve feature extraction by reducing computational burden.

A crucial technology in EfficientNet is its usage of the compound scaling approach that adapts the network's dimensions in a balanced approach. The conventional method frequently scales only one dimension, namely, width or depth, resulting in efficiency loss. However, EfficientNet scales every three dimensions concurrently, enabling the network to develop in size while remaining effective. An additional crucial characteristic of EfficientNet is its capability of generalizing through various agricultural image modalities. Where primarily intended for image detection challenges on larger, usual databases, EfficientNet's structure enables it to be fine-grained for particular challenges, such as wheat seed quality classification, with comparatively minimal changes. This flexibility is essential in agricultural imaging, where the features and quality of imagery may differ considerably based on the modality employed. EfficientNet is crucial in the image classification tasks, providing a strong integration of adaptability, accuracy, and efficiency. The study in the region continues to develop and remains at the forefront in agricultural image detection.

3.2.2. SqueezeNet

The structure of SqueezeNet is a compact and practical DL methodology. The lightweight framework is exceptionally relevant in limited resources. The pre-processed image data D_{no} is passed to SqueezeNet method that employs its simplifed yet efficient framework to rapidly recognize crucial features [23]. The structure of SqueezeNet comprises various convolutional layer, starts with "conv1" and concludes with "convl0" The method contains nine components that significantly increase proficiency using optimizer. To improve computation efficacy, max-pooling operations with dual stride were employed in succeeding "convl", "fire4", "fire8" and "convl0". The pooling layer provides the feature selection and aids to lessen the dimension of inputting data. Furthermore, a layer of dropout succeeds "fire9" to standardize the method and uphold over-ftting. The "conv10" layer is altered to decrease the overall count of filters to two, equivalent to binary classification. The traditional SqueezeNet method still encounters computation tasks.

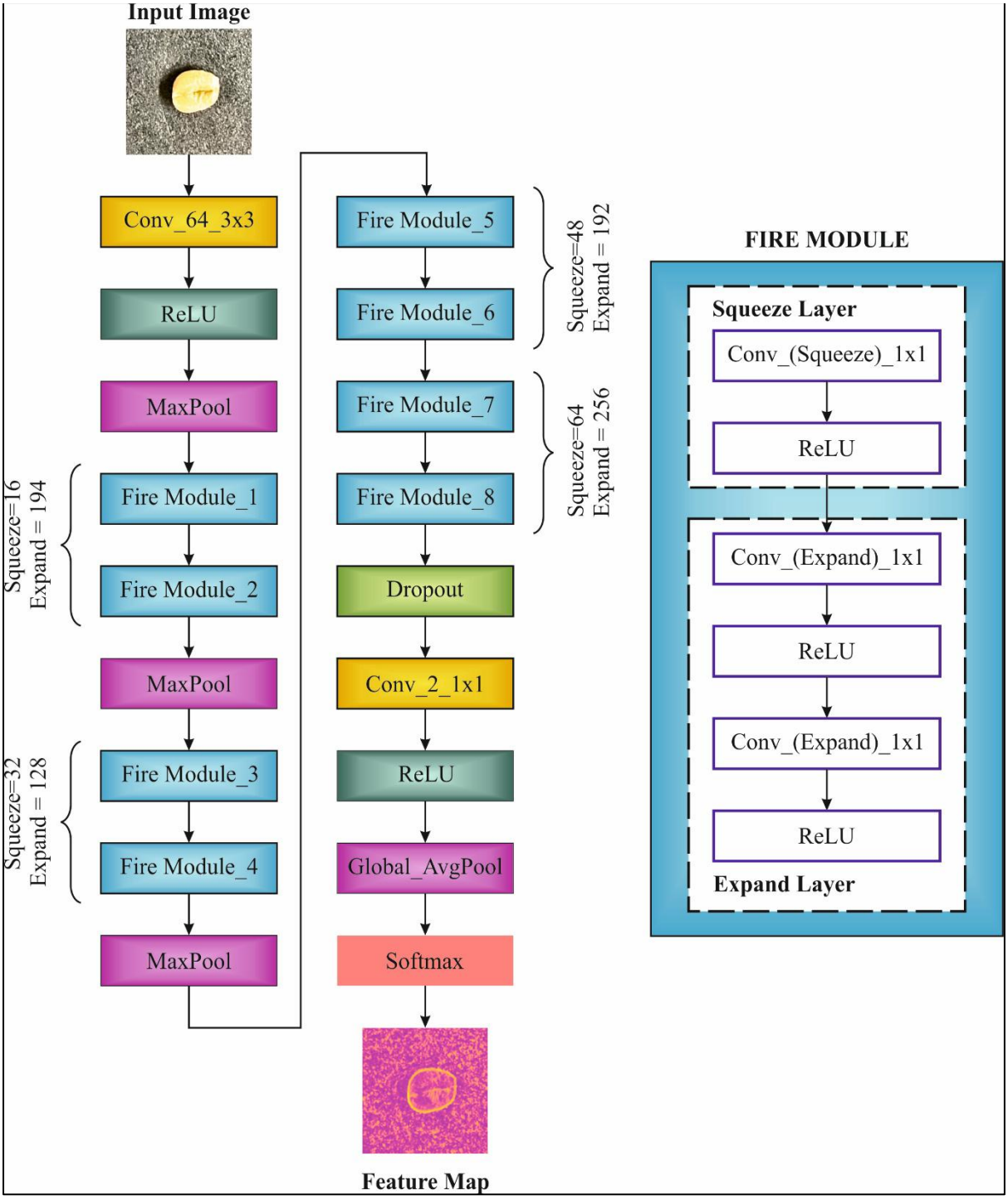

Fig. 2. Structure of SqueezeNet

In response to these restrictions, integrating Deep CNN (DCNN) with SqueezeNet creates a novel structure that diminish computation overload while enhancing the outcome. This incorporation assures that the method upholds greater efficacy while managing the problem of vanishing gradient, frequently viewed in deeper convolutional techniques. The entire structure of DCNN and its elements are specified. Fig. 2 represents the structure of SqueezeNet.

Convolutional Layer (Conv Layer): It is the major component of CNN. The kernel collection occurs, and their parameters are required to be exposed in the procedure of training.

Activation Function of ReLU: An activation function is extensively leveraged within CNN that choosily stimulates neurons, enhancing learning efficacy while maintaining gradient vanishing.

Scale dot product: It transmits an input query and key to the vector area where maximal values were attained for appropriate pairing using their inner product.

Sigmoid function: It was mainly employed to choose which values are approved as outcome and which ones shouldn't.

Enhanced stochastic mixed Lp layer: Multi-nomial distribution has been employed by Stochastic pooling to picks a random value. Primarily, the probability p_i was evaluated for each section J by regulating an activation in the area. While $p = 1, A_i$ implies feature value at position i in pooling area J,λ generates a decision on utilizing max or average pooling.

$$S_{Jnew} = [A_L * S_J] \quad (2)$$

$$LP(p1 \ldots . . p|rj|) \quad (3)$$

$$S_J = \left(\lambda maeA_i \; i \in r_J \; + (1-\lambda) \frac{1}{|r_J|} \sum_{i \in r_J} \; _- \right) \quad (4)$$

$$\text{p\_i=A\_i/\_K}\in\text{rj\^{}A\_k} \quad (5)$$

3.2.3. CapsNet

CapsNet is a sophisticated DL approach initiated from CNN within a unique computation unit known as capsule. Every capsule leverages a cluster of neurons to learn a huge number of features for particular entity exist in imagery comprising the instantiation parameters and existing likelihood [24]. The CapsNet accepts an informative outcome of vector rather than scaling value for feature expression and substitutes pooling operation in CNN through dynamic routing for encoder of spatial relation attributes. Consequently, highly expressive for entities and extremely beneficial to spatial knowledge mining.

Particularly, every capsule have vector inputs and outcomes. In capsule j, its input s_i denotes weighted addition of projected vector $\widehat{u_{j|\iota}}$ from outcome u_i of preceding capsule i.

$$s_j = \sum_i \; _{-j-\widehat{|\iota}} \widehat{u\_J|\iota} = W_{ij} u_j \quad (6)$$

Here, W_{ij} signified the equivalent weight from matrix W, and c_{ij} implies coupling co-efficient generated by dynamic routing. Afterwards, the outcome vector v_j is influenced by non-linear squashing function.

$$v_j = \frac{||s_j||^2}{1 + \|s_j\|^2} \frac{s_j}{\|s_j\|^2} \quad (7)$$

Now its length indicates existing likelihood of targeted entity and its position defines numerous aspects of entity.

A distinctive CapsNet has the structure of autoencoder, with the encoder composed by few convolutional layers, an initial layer of capsule, layer of entity capsule and the decoder formed by numerous fully connected (FC) layers. The convolutional layer is employed for eliminating an essential attributes and create appropriate inputs. The initial capsule layer learning the entity-related attributes in the vector expression attribute. The entity capsule layer, also called the class capsule layer, with every capsule generating a vector relevant on specific class. Although the FC layer inside decoder were employed for rebuilding the input depending upon the outcome of vector and promoting the encoder to acquire highly instructive attributes from pre-processed images.

3.2.4. Multi-Model Feature Fusion

The proposed AWSVCPA-ODL model integrates a hybrid multi-model feature fusion framework to derive a wide-ranging and discriminative visual representation of wheat seed imagery. Meanwhile, seed varieties frequently vary subtly in texture, surface morphology, and shape, depends on single method can limit the discriminative ability of eliminated attributes. Consequently, 3 different deep feature extractors: EfficientNet, SqueezeNet, and Capsule Network are conjointly leveraged to acquire complementary features from the pre-processed image. Assume that pre-processed wheat seed imagery is represented as I. Every method eliminates higher-level feature embedding is given:

$$F_E = EfficientNet(I), F_S = SqueezeNet(I), F_C = CapsuleNet(I) \quad (8)$$

Where, F_S depicts lightweight convolution of SqueezeNet's and fire-module-based attributes, F_E depicts EfficientNet's multi-scale CNN spatial attributes, and F_C indicates Capsule Network's pose-aware, viewpoint-invariant capsule features that acquires fine-grained spatial relations vital for varietal distinction.

To construct a unified model, the 3 embeddings were combined by channel-wise concatenation:

$$F_{concat} = [F_E \parallel F_S \parallel F_C] \quad (9)$$

Since concatenation rises dimensionality, a fully connected projection layer is employed to condense and normalize the fused representation:

$$F_{fusion} = W \cdot F_{concat} + b \quad (10)$$

The resultant fused feature vector F_{fusion} effectively integrates multi-scale CNN features, lightweight structural components, and capsule-based spatial agreement patterns. This enriched representation intensifies the discriminative ability of the model, allowing strong wheat seed varietal recognition and dependable purity evaluation.

3.3. Varietal and Purity Classification Strategy

In the classification step, a hybrid DL model is developed for effectively detecting and classifying wheat variety and its purity. Bi-GRU is employed in this study for wheat variety classification for purity assessment. Bi-GRU comprises a forward GRU component and a reverse GRU component. GRU includes reset and update gates [25]. The framework of the gate can select to save an image that resolves the issue of RNN explosion or gradient disappearance.

For time t, the formulation of the GRU cell state has been specified.

$$r_t = \sigma(w_r \cdot [h_{t-1}, x_t] + b_r) \quad (11)$$

$$z_t = \sigma(w_z \cdot [h_{t-1}, x_t] + b_z) \quad (12)$$

$$\widetilde{h_t} = tanh\,(w_h \cdot [r_t * h_{t-1}, x_t] + b_h) \quad (13)$$

$$h_t = (1 - z_t) * h_{t-1} + z_t * \tilde{h} \quad (14)$$

Here, $\cdot$ indicates dot product, σ represent the sigmoid function, w_r, w_z, w_h implies weighted matrices and b_r, b_z, b_h refers to biased parameters, x_t denotes the input vector of tth time , and h_t signifies hidden layer (HL) of preceding t time. z_t indicates an upgrading gate employed to regulate the impacts of preceding unit's HL outcome on existing state of unit. The maximal value of upgrade gate, the higher impacts of preceding unit of HL outcome on existing unit state. r_t indicates resetting gate is leveraged to manage the significance of h_{t-1} to $\tilde{h}_t$.The minimal value of resetting gate, the higher level to which the HL data of preceding unit was ignored. $\widetilde{h_t}$ indicates data that require to be upgraded in existing component. In this instance, the outcome is corresponding to LSTM, the architecture of GRU is easier than LSTM and the speed of training is quicker.

The BiGRU system contains forward GRU and reverse GRU components. The HL of forward GRU component is stated $\overrightarrow{h_t}$ and HL of reverse GRU component has been specified $h_t\ ^{\leftarrow}$. The HL outcomes of unidirectional GRU at time t were attained. The HL outcome of Bi-GRU at time t is spliced by HL outcome of forward GRU and reverse GRU components.

$$\overrightarrow{h_t} = GRU\big(x_t, \overrightarrow{h_{t-1}}\big) \quad (15)$$

$$h_t\ ^{\leftarrow} = GRU(x_t,\ h_{t-1}\ ^{\leftarrow}) \quad (16)$$

$$h_t = \big[\overrightarrow{h_t},\ h_t\ ^{\leftarrow}\big] \quad (17)$$

The goal of BiGRU is to acquire the attributes of a sequence. The Bi-GRU method is intricate to acquire significant data from sequences. Consequently, the Bi-GRU network acquires the attributes, and presents a self-attention mechanism to further acquire significant data. It can allocate weight to significant data, and precisely acquire semantical sequence.

Self-attention mechanism was considered a map of query to order of key-value pairs. To deliberate a self-attention mechanism cannot acquire substantial attributes from various levels and angles, it is essential to employ the multi-head attention mechanism. This mechanism mapping an input to numerous vector spaces and calculates the depiction of image in vector space.

$$m(h_t) = concat\big(score_1(h_t), score_2(h_t), \ldots., score_h(h_t)\big)W^O \quad (18)$$

Here, h denotes repeat number, h_t represents HL outcome of Bi-GRU, $score_i$ indicates the outcome of i^{th} self-attention mechanism.

$$score_i(h_t) = attention\left(h_t W_i^Q, h_t W_i^K, h_t W_i^y\right) \quad (19)$$

Now, W_i^Q, W_i^K, W_i^v and W^O implies parameter matrices that is employed mapping input h_t to diverse vector spaces. The dimension of parameter matrix hold $W_i^Q \in R^{d\times d_Q}, W_i^K \in R^{d\times d_Q}, W_i^v \in R^{d\times d_V}, W^O \in R^{hd_V\times d}$, correspondingly. Here, d signifies the outcome vector size of Bi-GRU network HL, d_Q and d_v refers to dimension of vector space.

$$attention\ (Q,K,V) = softmax\left(\frac{QK^T}{\sqrt{d}}\right) \quad (20)$$

Now, $\sqrt{d}$performs the part of scaling modifications. The HL outcome of BiGRU at tth time is described $H_t = m(h_t)$. The outcome order of BiGRU is $H = (H_1, H_2, \dots, H_n)$ also the outcome of layer.

3.4. Model Optimization

The Adabelief hyperparameter optimizer is applied to further improve the performance of classification model (SA-BiGRU). Adabelief is an optimization, depending on an adaptive learning rate approach is widely applied for parameter tuning tasks. It is intended to tackle the issue of training efficacy connected with small-batch datasets. The basis of Adabelief resides its update rule [26]. Traditional optimizer namely Adam employs momentum terms and second-order moment estimates. Conversely, Adabelief presents an innovative notion of "belief" that relies on the square ratio of gradient to its historical mean. Particularly, this ratio surpasses 1, Adabelief inclines to place in the existing gradient data. In contrast, while the ratio is lesser than or equal to 1, it relies more on past data. This dynamic modification allows Adabelief to discover the solution area more effectually while managing non-convex concerns.

The Adabelief model comprises the succeeding 4 stages:

(1) Initialization

The rate of learning α, together with dual parameters β_1 and β_2 is initialized. Furthermore, the first-order moment approximation m_t and the second-order moment approximation s_t are also initialized.

(2) Gradient update

For every parameter ω, the gradient at time t step is g_t .The approximation of first-order moment and the second-order moment were evaluated.

$$m_t = \beta_1 m_{t-1} + (1-\beta_1) g_t \quad (21)$$

$$s_t = \beta_2 s_{t-1} + (1-\beta_1) \setminus g_t - m_t \quad (22)$$

(3) Bias correction

Bias correction is implemented to the first-order moment and the second-order moment:

$$\widehat{m} = \frac{m_t}{1-\beta_1^t} \quad (23)$$

$$\hat{s}_t = \frac{s_t}{1-\beta_2^t} \quad (24)$$

(4) Parameter update

The rule for upgrading parameters ω is given.

$$\omega_t = \omega_{t-1} - \frac{\alpha\widehat{m}}{\sqrt{\widehat{s_t}}E} \quad (25)$$

Here, E denotes smaller constant and utilized to uphold division by zero errors.

3.5. Assessment Metrics

Evaluation metrics are employed for evaluating the limitations and robustness of the suggested model, allowing crucial modifications to attain optimal performance. The various performance measures are used TP, TN, FP, FN signifies True Positives, True Negatives, False Positives and False Negatives.

Accuracy is the fraction of forecasts correct examples to the total amount of examples:

$$Accuracy = \frac{TP + TN}{TP + TN + FP + FN} \quad (26)$$

Precision is the fraction of TP forecasts to the total positive forecasts:

$$Precision = \frac{TP}{TP + FP} \quad (27)$$

Recall is the fraction of TP forecasts to the total real positive cases:

$$Recall = \frac{TP}{TP + FN} \quad (28)$$

F-score is nothing but the harmonic mean of recall and precision, balancing the dual parameters:

$$F - score = 2 \times \frac{Precision \times Recall}{Precision + Recall} \quad (29)$$

MCC is a measure of quality of binary classifiers that is seen as reliable even with imbalanced categories. It is effectively a CC among the monitored and forecast binary classifiers.

$$MCC = \frac{TP \cdot TN - FP \cdot FN}{\sqrt{(TP + FP)(TP + FN)(TN + FP)(TN + FN)}} \quad (30)$$

. Findings and Interpretation

In this part, the performance evaluation of the AWSVCPA-ODL model is examined under the Varietal purity of wheat seeds dataset [27]. The dataset consists of 1125 images under 3 classes such as Urooj-22, Akbar-19, and Dilkash-20 as shown in Table 2. All varieties is signified by 125 images, leading to a total of 375 images through the 3 varieties. The images are taken employing an RGB DSLR camera and later standardized to a size of 256x256 pixels. The camera is placed parallel to the path of the seeds, assuring a constant perception. To improve variability, the wheat seeds are taken under natural light. This dataset may help for studying the wheat seed quality analysis and classification. Fig. 3 represents the flow diagram of seed image classification. Fig. 4 depicts the sample images of three variety names. The preprocessed, feature maps and GradCAM sample images are shown in Fig. 5.

Table 2 Detail of dataset

"Variety No."	**"Variety Name"**	**"Total No. of Images"**
"1"	"Akbar-19"	"375"
"2"	"Dilkash-20"	"375"
"3"	"Urooj-22"	"375"
"Total"	**125**	**1125**

Akbar-19: The wheat variety Akbar-19 has not only higher yield potential, climate re- resilience, rust resistance but also has higher zinc content (39 mg kg-1). The medium-sized, amber-colored oval seeds have a short brush but a uneven surface with an intermediate groove. The seed's germ size is medium. The Akbar-19 seeds are heavier and larger than other seeds, which supports them growing more in the Pakistani climate. Akbar-19 wheat has extra grain plumpness that rises its popularity. Akbar-19 is a wheat seed variety known for its good grain quality, higher yield, and appropriateness for chapatti making. It has an optimizes development period, good water use efficiency, and uniform grain size. Akbar-19 also has a nutritional profile and boasts disease resistance.

Dilkash-20: Dilkash-20 is an accepted wheat variety, especially suggested for irrigated regions in Punjab, Pakistan. It boasts high yield potential and is resilient to yellow and brown rusts that making it appropriate for wider cultivation in the area. Dilkash-20 variety is medium-sized as well s rounder than Akbar-19. Its seed texture is uneven, like Akbar's but somewhat harsh. Its color is light brown. It is of higher quality, with a good percentage of gluten, protein, and starch, making it ideal to create chapattis. Depend on the resistance genes of adult plants, it takes a longer-lasting and efficient defense compared to yellow and brown rusts.

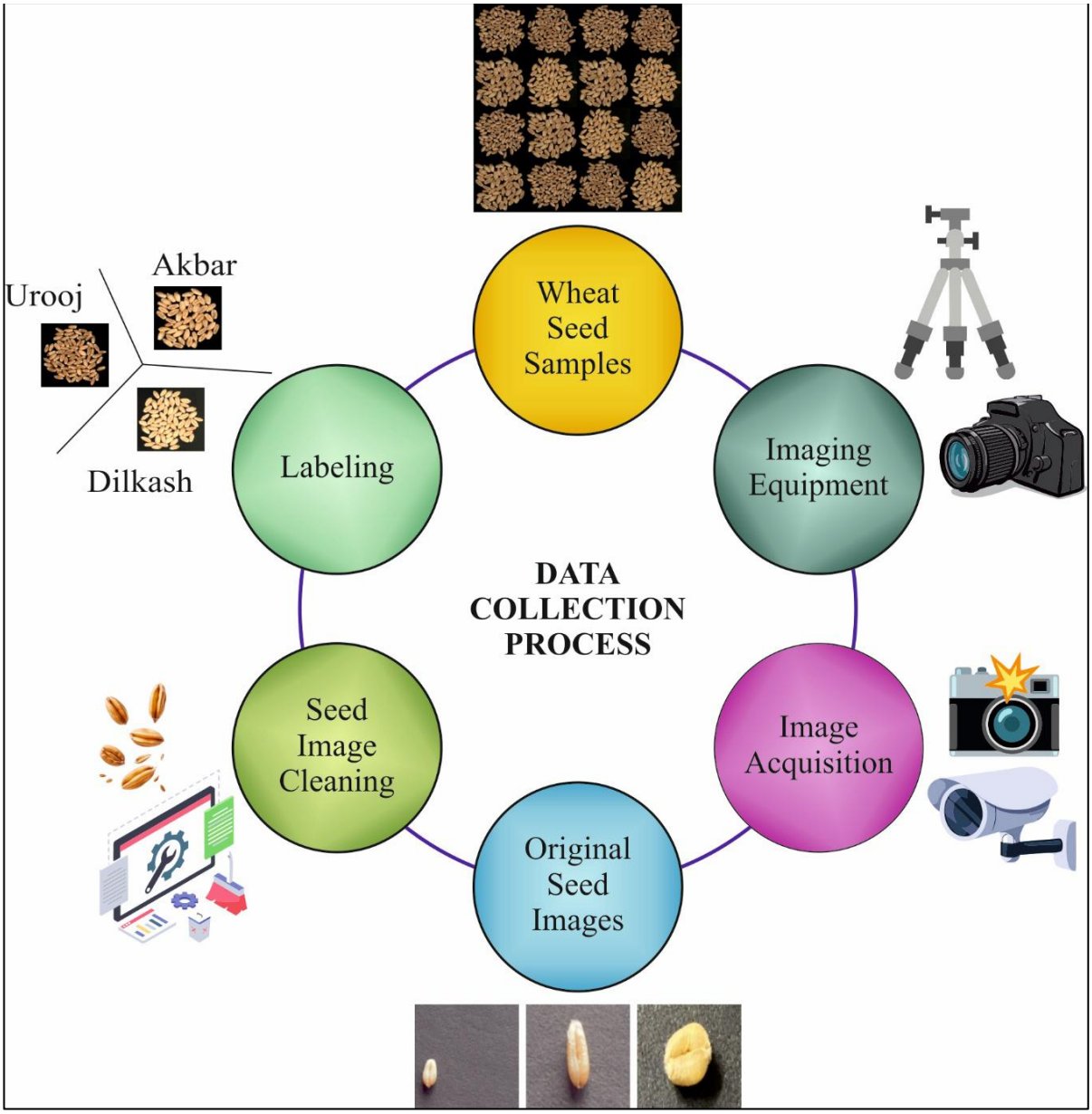

Fig. 3. Flow diagram of seed image classification

Urooj-22: Arooj-22 is a bread wheat variety appropriate for both rainfed as well as irrigated regions. It's known for its higher yield potential, especially in irrigated states, and its resistance to leaf and yellow rust. The Urooj-22 variety seeds are 7-8 mm longer, ovate and amber in colour. The width of the seed is 3–3.5 mm, which is thinner than Akbar-19. The medium size, and its opaque surface. Its 10 0 0-grain weight is 43g which is examined between the higher-yield wheat cultivars. The Urooj-22 variety is typically chosen in areas that need drought-resistant crops.

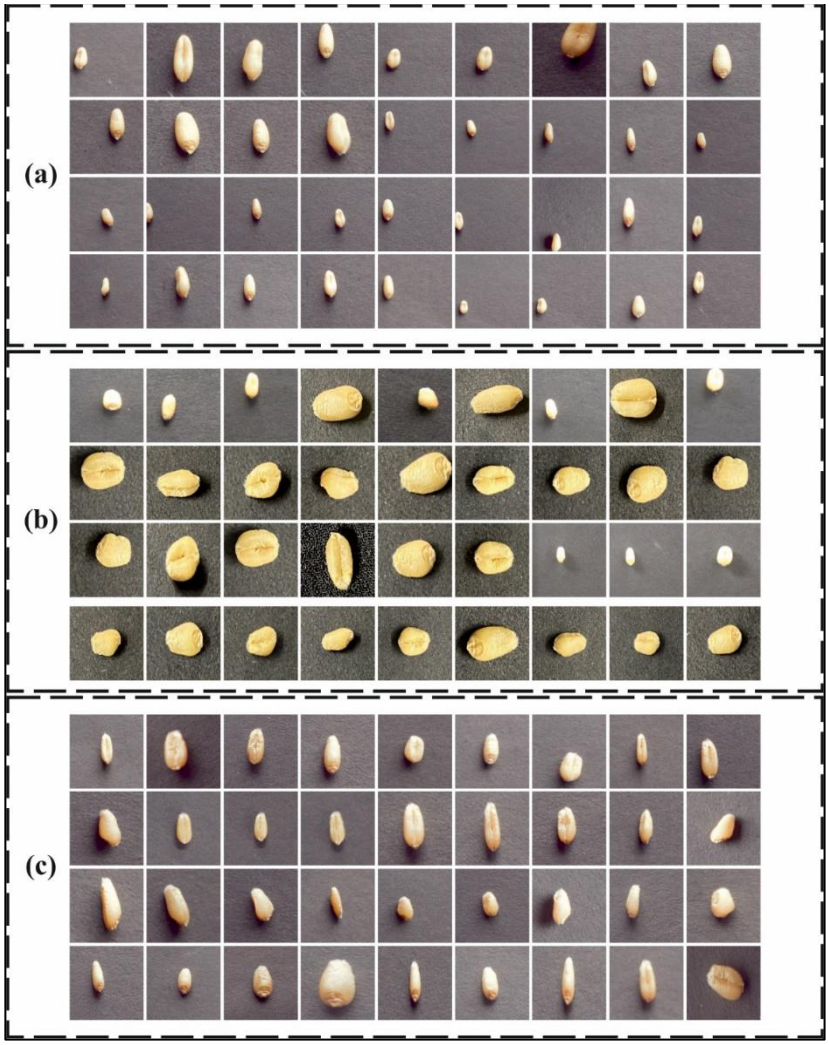

Fig. 4. Sample images of (a) Urooj, (b) Akbar, and (c) Dilkash

Fig. 6 depicts a classifier outcome of three varieties such as Akbar-19, Dilkash-20, and Urooj-22, which are assessed through multiple epochs (500 to 3000) using 5 key metrics. Overall, the outcomes display a clear rising tendency for every technique as the number of epochs rises, suggesting enhanced convergence and learning. Akbar-19 constantly accomplishes higher scores through most metrics, particularly at the highest epochs, reflecting robust generalization and stability. Dilkash-20 keep on closely with competitive performance that gradually enhances with training. Urooj-22 exhibits comparatively lesser values in previous epochs but proves notable enhancement as training progresses. By 3000 epochs, each three methods gain their peak performance, with narrowed variances through metrics, indicating the positive effect of expanded training on model reliability and robustness.

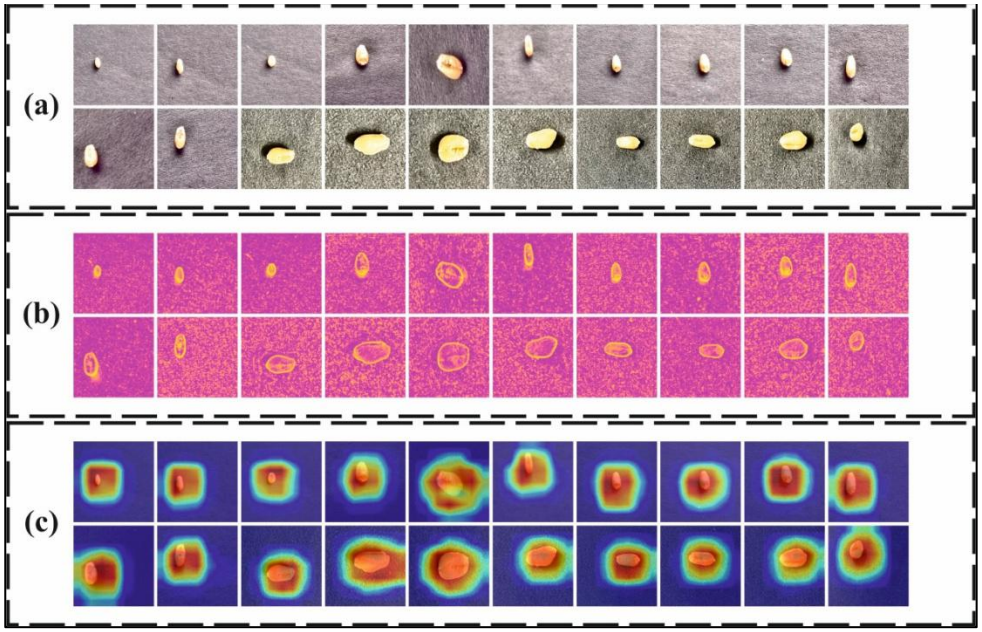

Fig. 5. Sample images of (a) Pre-processed, (b) Feature maps, and (c) GradCAM

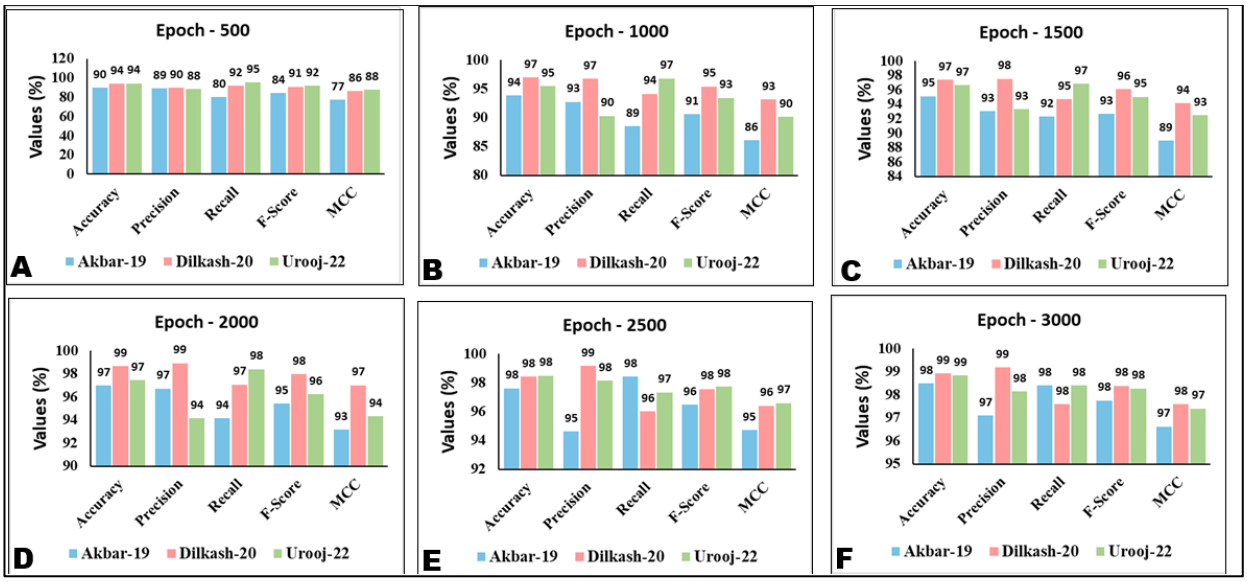

Fig. 6. Classifier outcome of AWSVCPA-ODL model under (A-F) Epochs 500 – 3000

Table 3 and Fig. 7 shows the classifier outcome of AWSVCPA-ODL approach under various epochs. Under 500 epoch, the proposed AWSVCPA-ODL method reaches average $accur_y$, $preci_n$, $recal_l$, F_{score}, and MCC of 92.71%, 89.08%, 89.07%, 88.94%, and 83.65%, respectively. Also, under 2000 epoch, the proposed AWSVCPA-ODL method accomplishes average $accur_y$, $preci_n$, $recal_l$, F_{score}, and MCC of 97.69%, 96.59%, 96.53%, 96.54%, and 94.83%, respectively. Besides, under 2500 epoch, the proposed AWSVCPA-ODL method attains average $accur_y$, $preci_n$, $recal_l$, F_{score}, and MCC of 98.16%, 97.30%, 97.24%, 97.25%, and 95.90%, respectively. Moreover, under 3000 epoch, the proposed AWSVCPA-ODL model obtains average $accur_y$, $preci_n$, $recal_l$, F_{score}, and MCC of 98.76%, 98.14%, 98.13%, 98.13%, and 97.21%, respectively.

Table 3 Classifier outcome of AWSVCPA-ODL model under various epochs

Classes	Epochs	$Accur_y$	$Preci_n$	$Recal_l$	F_{score}	MCC
Akbar-19	500	90.04	89.02	80.00	84.27	77.25
	1000	93.87	92.74	88.53	90.59	86.09

	1500	95.11	93.01	92.27	92.64	88.98
	2000	96.98	96.71	94.13	95.41	93.17
	2500	97.60	94.62	98.40	96.47	94.70
	3000	98.49	97.11	98.40	97.75	96.62
Dilkash-20	500	93.78	89.82	91.73	90.77	86.09
	1000	96.98	96.71	94.13	95.41	93.17
	1500	97.42	97.53	94.67	96.08	94.18
	2000	98.67	98.91	97.07	97.98	97.00
	2500	98.40	99.17	96.00	97.56	96.40
	3000	98.93	99.19	97.60	98.39	97.60
Urooj-22	500	94.31	88.40	95.47	91.79	87.60
	1000	95.47	90.30	96.80	93.44	90.11
	1500	96.62	93.32	96.80	95.03	92.51
	2000	97.42	94.13	98.40	96.22	94.32
	2500	98.49	98.12	97.33	97.72	96.59
	3000	98.84	98.14	98.40	98.27	97.40
Global Values	500	92.71	89.08	89.07	88.94	83.65
	1000	95.44	93.25	93.16	93.14	89.79
	1500	96.39	94.62	94.58	94.58	91.89
	2000	97.69	96.59	96.53	96.54	94.83
	2500	98.16	97.30	97.24	97.25	95.90
	3000	98.76	98.14	98.13	98.13	97.21

Fig. 8 presents the training (TRAN) and validation (VALD) accuracy of AWSVCPA-ODL model under Epoch 3000. Both curves slowly converge and gradually rise, which implies that the technique is learning effectually. The VALD accuracy constantly remains slightly superior than the TRAN accuracy, implying that the method is not overfitting and generalizes well to unseen data. The fluctuations in accuracy are expected

because of the difficulty of the task, but the total increasing tendency proves stronger performance and model stability.

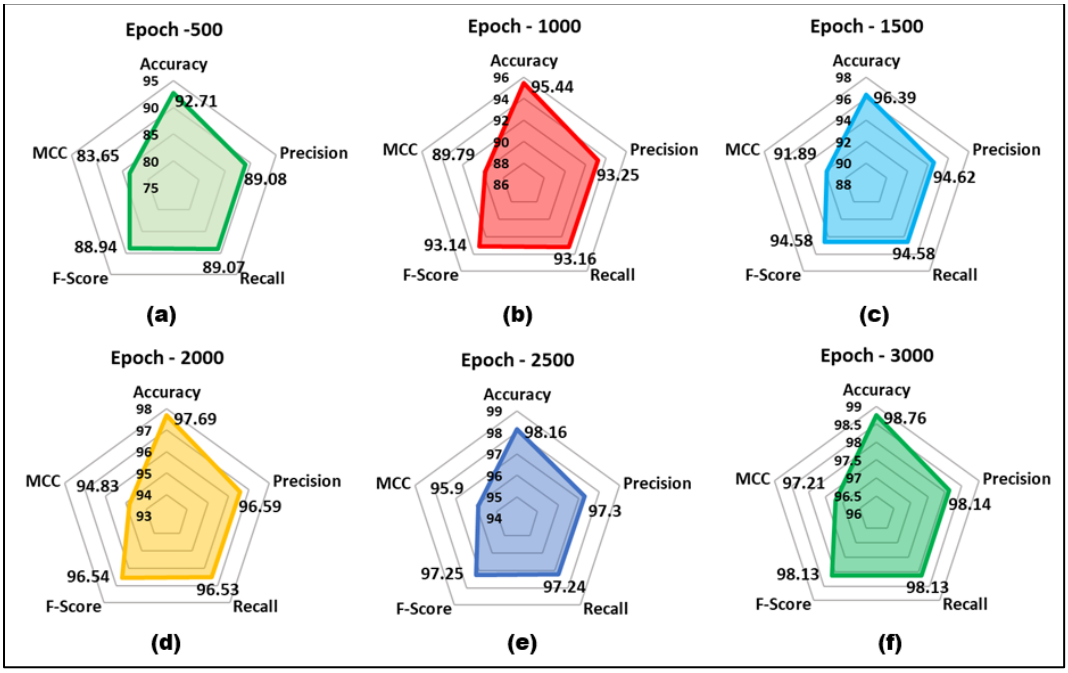

Fig. 7. Average values of AWSVCPA-ODL model (a-f) Epochs 500 - 3000

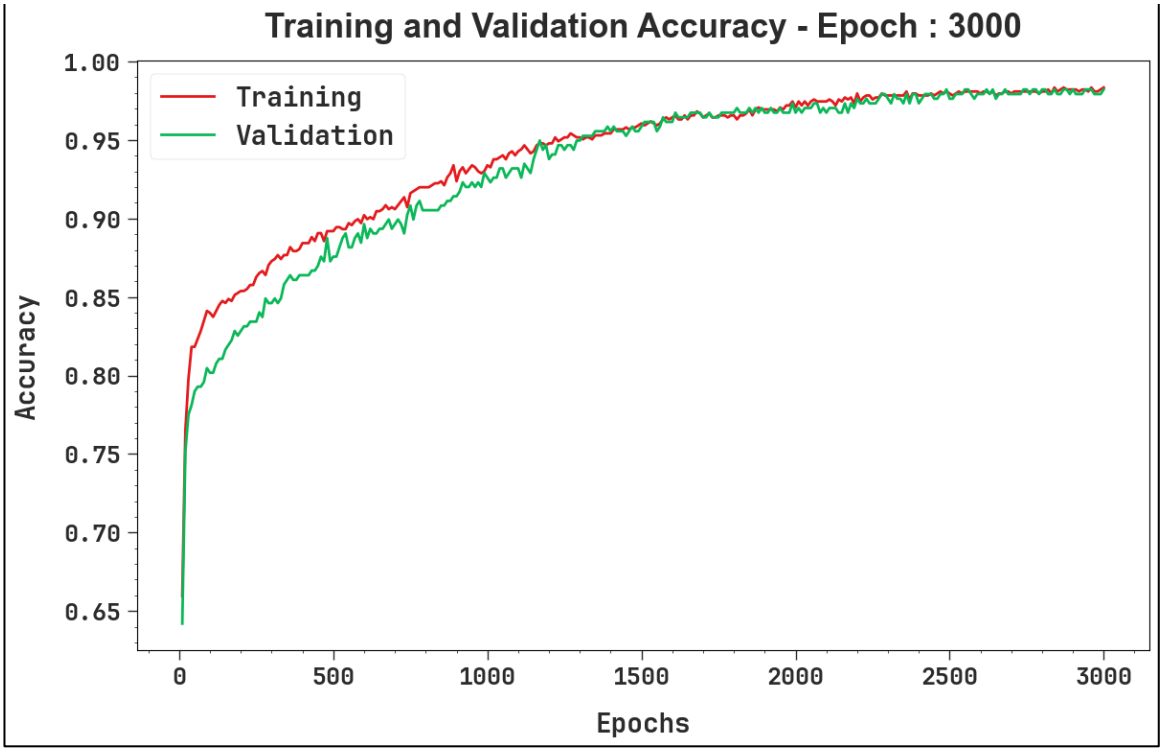

Fig. 8. Accuracy curve of AWSVCPA-ODL algorithm on Epoch 3000

Fig. 9 represents the TRAN and VALD loss of AWSVCPA-ODL model under Epoch 3000. Both curves reveal a constant reducing tendency, implying that the system efficiently minimizes error throughout learning. The VALD loss stays somewhat smaller than the training loss across most epochs, implying good generalizes and no signs of overfitting. Though some fluctuations are monitored is becoming progressively steady and more constant.

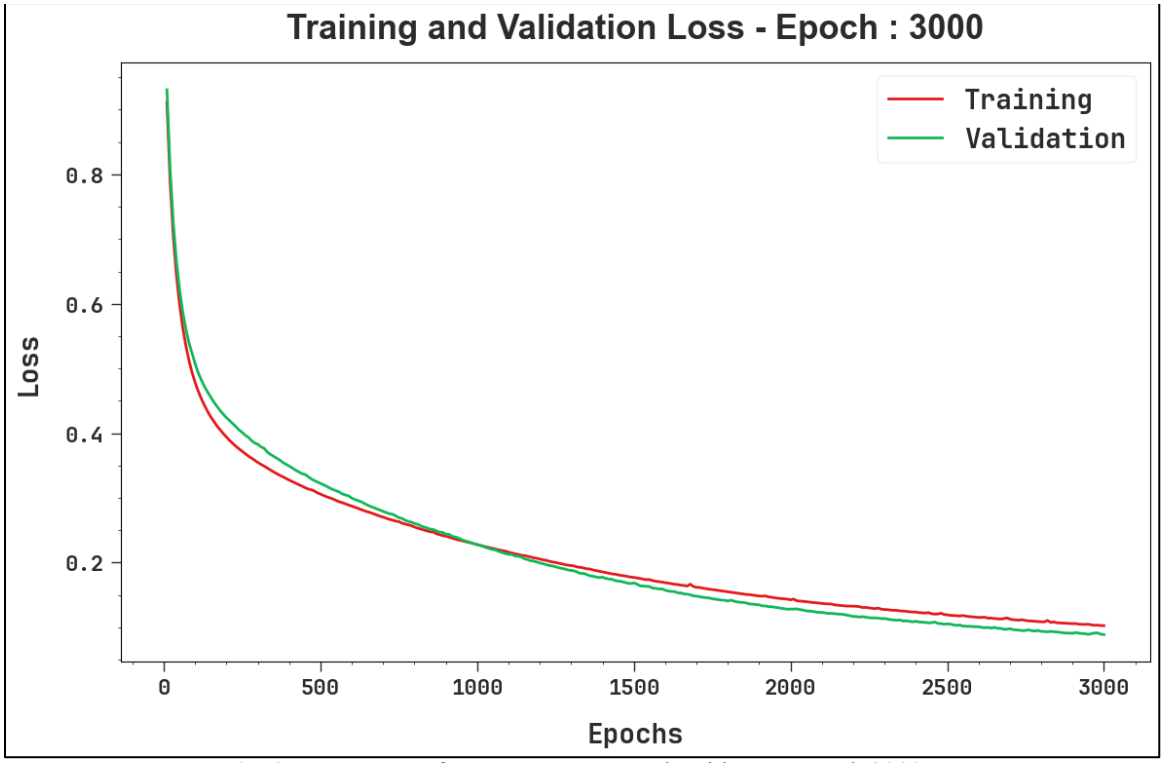

Fig. 9. Loss curve of AWSVCPA-ODL algorithm on Epoch 3000

Fig. 10 reveals the Precision–Recall (PR) and ROC curves of AWSVCPA-ODL model under Epoch 3000. This figure exemplifies the stronger classification performance of the three models. The Fig. 10a portrays the PR curve, each model exhibit higher precision through almost the whole recall range, suggesting their capability of correctly identifying positive samples with lesser false alarms. Likewise, the Fig. 10b proves ROC curve that every three models accomplish near-perfect true positive rates while upholding very lower false positive rates. The tight overlap of the curves in both plots implies that the models perform comparably well at the phase, attaining outstanding discrimination and strong prediction ability after 3000 training epochs.

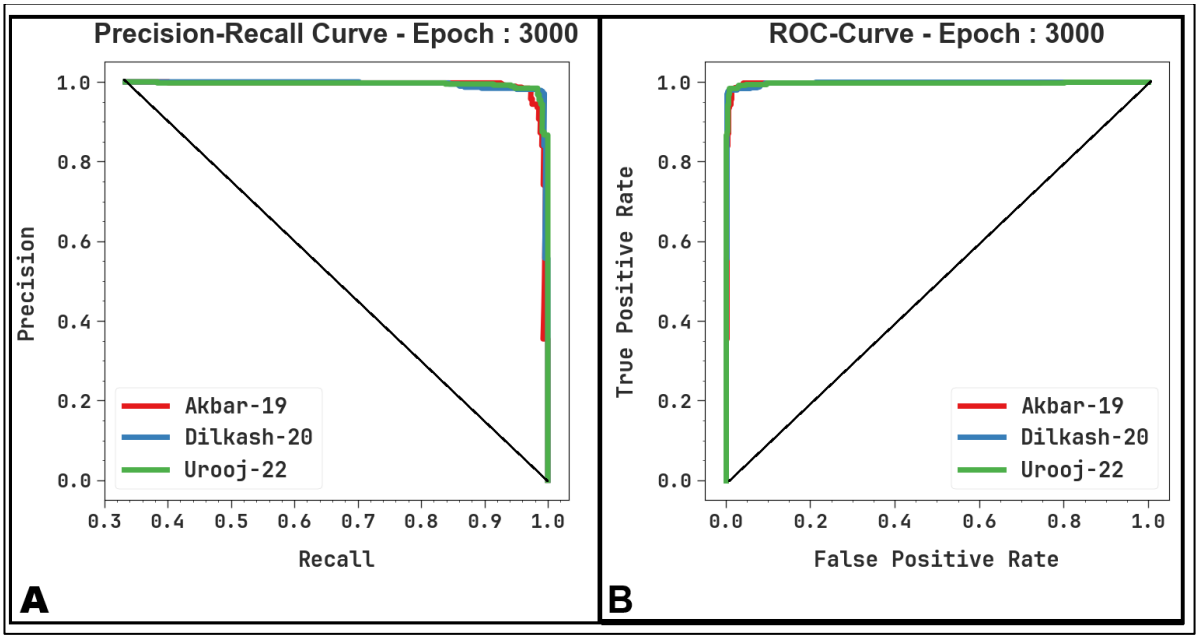

Fig. 10. PR and ROC curves of AWSVCPA-ODL model under Epoch 3000

Table 4 and Fig. 11 show the comparative outcomes of AWSVCPA-ODL model with existing model under several metrics and error rate [17, 28]. The ResNet18 approach has attained inferior $accur_y$, $preci_n$, $recal_l, and\ F_{score}$ of 94.97%, 92.93%, 96.89%, and 91.56%, respectively. Meanwhile, the DenseNet121method has achieved lower $accur_y$, $preci_n$, $recal_l, and\ F_{score}$ of 95.44%, 94.98%, 93.01%, and

90.05%, respectively. Likewise, the GoogLeNet method has got minimal $accur_y$, $preci_n$, $recal_l$, $and\ F_{score}$ of 93.80%, 92.27%, 92.01%, and 95.46%, respectively. Also, the SECA-DenseNet121 method has gained lesser $accur_y$, $preci_n$, $recal_l$, $and\ F_{score}$ of 96.53%, 93.83%, 92.35%, and 95.22%, respectively. In addition, the proposed AWSVCPA-ODL model has achieved superior $accur_y$, $preci_n$, $recal_l$, $and\ F_{score}$ of 98.76%, 98.14%, 98.13%, and 98.13%, respectively. Under error rate, the proposed AWSVCPA-ODL model has reached minimal error rate of 1.24%, whereas the existing models such as ResNet18, DRNet, DenseNet121, GC-DRNet, GoogLeNet, Vgg16, and SECA-DenseNet121 have accomplished greater error rate of 5.03%, 3.36%, 4.56%, 2.93%, 6.20%, 9.29%, and 3.47%, respectively.

Table 4 Comparative analysis of AWSVCPA-ODL technique with existing models

Models	$Accur_y$	**Error Rate**	$Preci_n$	$Recal_l$	F_{score}
ResNet18	94.97	5.03	92.93	96.89	91.56
DRNet	96.64	3.36	95.42	96.20	97.00
DenseNet121	95.44	4.56	94.98	93.01	90.05
GC-DRNet	97.07	2.93	95.78	91.39	95.94
GoogLeNet	93.80	6.20	92.27	92.01	95.46
Vgg16	90.71	9.29	95.21	91.80	96.71
SECA-DenseNet121	96.53	3.47	93.83	92.35	95.22
AWSVCPA-ODL	98.76	1.24	98.14	98.13	98.13

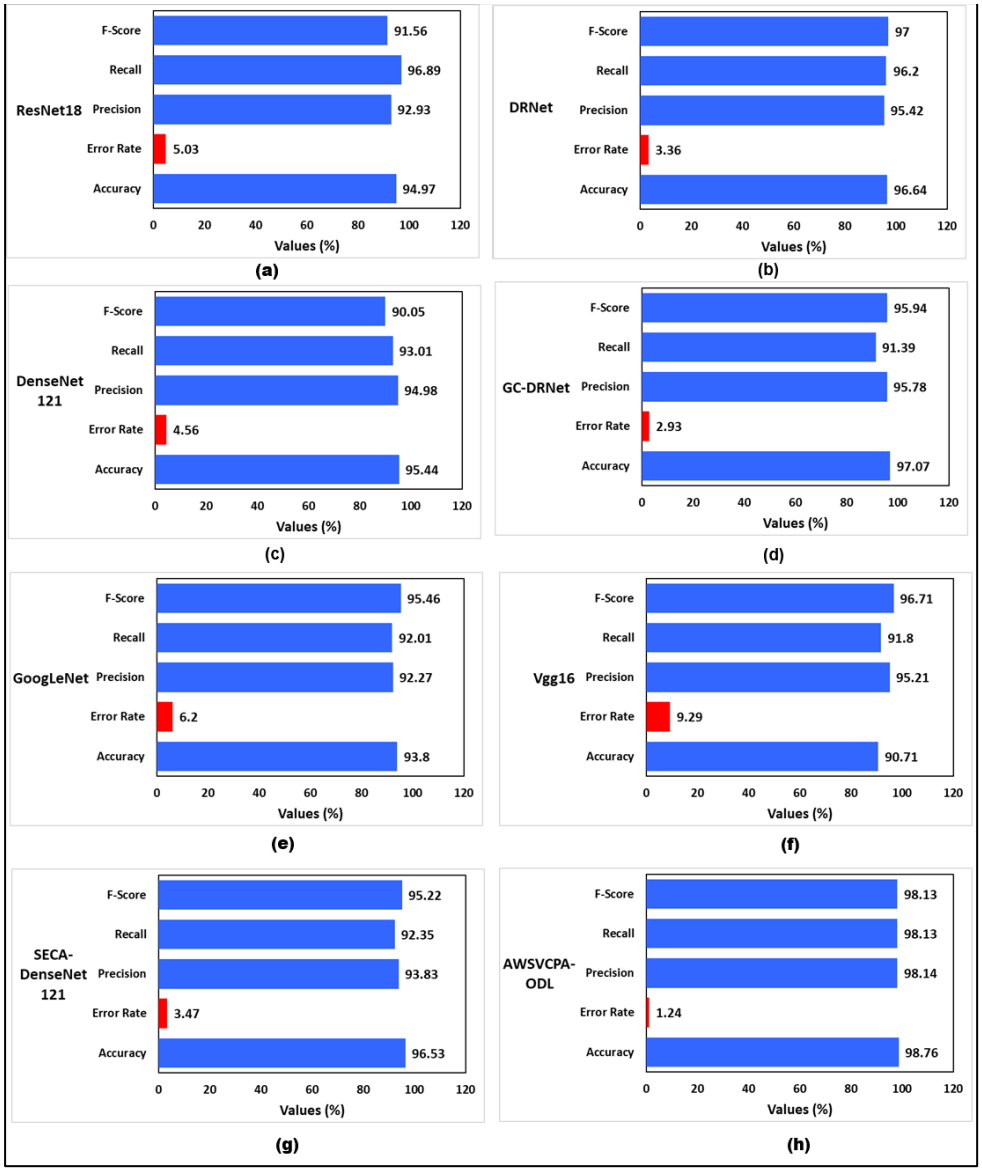

Fig. 11. Comparative outcomes of AWSVCPA-ODL methodology with existing approaches

Table 5 display the computational efficiency of AWSVCPA-ODL model. Under parameter, the proposed AWSVCPA-ODL model has attained lower parameter of 6.55MB, whereas the existing systems ResNet18, DRNet, DenseNet121, GC-DRNet, GoogLeNet, Vgg16, and SECA-DenseNet121 have obtained greater parameter of 44.59MB, 10.30MB, 11.65MB, 82.30MB, 65.70MB, 70.80MB, and 84.50MB, correspondingly. Under FLOPs, the proposed AWSVCPA-ODL model has got minimal FLOPs of 0.067G, whereas the existing systems ResNet18, DRNet, DenseNet121, GC-DRNet, GoogLeNet, Vgg16, and SECA-DenseNet121 have gained maximal FLOPs of 1.82G, 0.87G, 2.77G, 38.02G, 9.70G, 107.22G, and 104.74G, correspondingly. Under frames, the proposed AWSVCPA-ODL technique has attained inferior frames of 10.05s, whereas the existing techniques ResNet18, DRNet, DenseNet121, GC-DRNet, GoogLeNet, Vgg16, and SECA-DenseNet121 have achieved higher frames of 48.80s, 52.30s, 65.80s, 67.60s, 77.50s, 43.70s, and 22.30s, correspondingly.

Table 5 Computational efficiency of AWSVCPA-ODL model

Model	Parameter (MB)	FLOPs (G)	Frames per Second
ResNet18	44.59	1.82	48.80
DRNet	10.30	0.87	52.30
DenseNet121	11.65	2.77	65.80

GC-DRNet	82.30	38.02	67.60
GoogLeNet	65.70	9.70	77.50
Vgg16	70.80	107.22	43.70
SECA-DenseNet121	84.50	104.74	22.30
AWSVCPA-ODL	6.55	0.067	10.05

5. Conclusion

In this manuscript, a novel AWSVCPA-ODL framework is presented for precisely analyzing wheat seed images using CV and DL techniques, facilitating reliable varietal classification and robust purity assessment. Primarily, the proposed AWSVCPA-ODL methodology follows two phases of pre-processing: GF for noise removal and contrast enhancement process to enrich the input seed image quality for subsequent analysis. For feature representation, the proposed AWSVCPA-ODL system follows a feature fusion process integrating EfficientNet, SqueezeNet, and CapsNet. The SA-BiGRU is designed to accurately detect and classify wheat variety and its purity. To further enhance the performance of the SA-BiGRU architecture, Adabelief hyperparameter optimizer is leveraged. For guaranteeing the improved performance of the proposed AWSVCPA-ODL framework, comprehensive simulations were conducted on benchmark dataset. The obtained results highlighted the efficiency of proposed AWSVCPA-ODL system compared to other advanced techniques.

Data Availability Statement: The data that support the findings of this study are openly available at https://data.mendeley.com/datasets/w5248v9fk3/1, reference number [27].

References

1. Jamil, M., Ahmad, W., Sanwal, M. and Maqsood, M.F., 2025. Gene editing and GWAS for digital imaging analysis of wheat grain weight, size and shape are inevitable to enhance the yield. *Cereal Research Communications*, pp.1-20.
2. Kurmanbayeva, M., Rašeta, M., Sarsenbek, B., Kusmangazinov, A., Zhumagul, M., Karabalayeva, D., Altybayeva, N., Gafforov, Y. and Toishimanov, M., 2025. Comparison of fatty acids and amino acids profiles of the selected perennial and annual wheat varieties from Kazakhstan. *Natural product research*, *39*(13), pp.3627-3632.
3. Wang, W., Zou, J., Zhang, Y., Niu, L., Yu, L., Wang, Z., Wang, F., Zhang, S. and Yang, X., 2025. Salinity stress phenotyping of wheat germplasm under multiple growth conditions and transcriptomic analysis of two wheat varieties contrasting in their salinity stress tolerance. *Plant Growth Regulation*, *105*(3), pp.739-757.
4. Mallem, H., 2025. Identifying Salt-Tolerant Durum Wheat Varieties (Triticum durum Desf.) Through Comprehensive Stress Analysis. *Russian Journal of Plant Physiology*, *72*(2), p.52.
5. Xiao, B., Hu, Y., Liu, Y., Jia, S., Zhang, T., Yin, S., Xiao, C., Jiang, J., Wang, L. and Yang, C., 2025. Physiological and transcriptional analysis provides insights into responses of a spring wheat variety to combination of salt and heat stresses. *Physiologia Plantarum*, *177*(2), p.e70154.
6. Karkhaneh, A., Salari, H., Cheghamirza, K. and Zarei, L., 2025. Agronomic and Molecular Identification of Drought-Tolerant Bread Wheat Varieties in Iran. *Journal of Plant Growth Regulation*, pp.1-12.
7. Abebe, A., 2025. Determinants of Adoption of Improved Wheat Varieties by Smallholder Farmers:-In Case of Angacha Woreda, Kembata Tembaro Zone, SNNPR. *Econ Dev Glob Mark*, *1*(1), pp.01-10.
8. Atreya, K., Gartaula, H.N. and Kattel, K., 2025. Household seed security: a case of maize and wheat seed systems in the mountains of Nepal. *Agricultural Systems*, *229*, p.104419.
9. Dama, A.Z., Simon, S.Y. and Tame, V.T., 2025. Analysis of Genotype by Environment Interaction in Bread Wheat (Triticum Aestivum L) For Breeding High-Yielding Varieties under Rain-Fed Conditions at Miango And Vom In Jos, Plateau State, Nigeria. *Journal of Applied Sciences and Environmental Management*, *29*(5), pp.1560-1567.
10. Yan, S., Zhao, X., Zhu, Q., Huang, M. and Guo, X., 2025. A method for constructing optical detection model of wheat seed purity based on sample generation and contrastive learning strategy. *Journal of Food Composition and Analysis*, *138*, p.107022.
11. Noori, A.F. and Mukhlif, R.Z., 2025. Molecular Profiling of Selected Aspergillus Species Parasitizing Stored Wheat Seeds in the Silos of Tikrit City, Iraq. *International Journal of Environmental Sciences*, *11*(1s), pp.88-96.
12. Adams, C.B., Neely, C. and Graebner, R., 2025. Yield variation, plasticity, adaptation, and performance ranking of winter wheat varieties across the environmental gradient of the US Pacific Northwest. *Crop Science*, *65*(1), p.e70018.
13. Yan, S., Zhao, X., Zhu, Q., Huang, M. and Guo, X., 2025. A method for constructing optical detection model of wheat seed purity based on sample generation and contrastive learning strategy. Journal of Food Composition and Analysis, 138, p.107022.
14. Gu, Y., Feng, G., Zhang, H., Hou, P., Wang, C., Chen, L. and Luo, B., 2025. Detection of Strigolactone-Treated wheat seeds via Dual-View hyperspectral data fusion and deep learning. Microchemical Journal, p.114295.

15. Janapati, M., Kakarla, M. and Tirumalasetty, B.S.S.K., 2025, March. Wheat Seed Quality Detection For Enhanced Agriculture using YOLOv8 and IOT. In 2025 6th International Conference on Recent Advances in Information Technology (RAIT) (pp. 1-6). IEEE.
16. Guo, X., Wang, J., Gao, G., Cheng, Z., Qiao, Z., Zhang, R., Ma, Z. and Wang, X., 2025. LWheatNet: a lightweight convolutional neural network with mixed attention mechanism for wheat seed classification. Frontiers in Plant Science, 15, p.1509656.
17. Xing, X., Liu, C., Han, J., Feng, Q., Lu, Q. and Feng, Y., 2023. Wheat-seed variety recognition based on the GC_DRNet model. Agriculture, 13(11), p.2056.
18. Zhao, X., Que, H., Sun, X., Zhu, Q. and Huang, M., 2022. Hybrid convolutional network based on hyperspectral imaging for wheat seed varieties classification. Infrared Physics & Technology, 125, p.104270.
19. Jin, S., Zhang, W., Yang, P., Zheng, Y., An, J., Zhang, Z., Qu, P. and Pan, X., 2022. Spatial-spectral feature extraction of hyperspectral images for wheat seed identification. Computers and Electrical Engineering, 101, p.108077.
20. Barysheva, N.N., Guner, M.V., Baryshev, D.D. and Pronin, S.P., 2020, August. Analysis of seed quality indicators based on neural network. In Journal of Physics: Conference Series (Vol. 1615, No. 1, p. 012022). IOP Publishing.
21. Ranjitha, K.V. and Pushphavathi, T.P., 2024. Analysis on improved Gaussian-Wiener filtering technique and GLCM based feature extraction for breast cancer diagnosis. *Procedia Computer Science*, *235*, pp.2857-2866.
22. Oyebanji, O.S., Apampa, A.R., Idoko, P.I., Babalola, A., Ijiga, O.M., Afolabi, O. and Michael, C.I., 2024. Enhancing breast cancer detection accuracy through transfer learning: A case study using efficient net. *World Journal of Advanced Engineering Technology and Sciences*, *13*(01), pp.285-318.
23. Bojarajulua, B., Tanwar, S. and Singh, T.P., 2025. Enhanced SqueezeNet model for detecting IoT-Bot attacks: A comprehensive approach. *MethodsX*, p.103499.
24. Zhai, H. and Zhao, J., 2024. Two-Stream spectral-spatial convolutional capsule network for Hyperspectral image classification. *International Journal of Applied Earth Observation and Geoinformation*, *127*, p.103614.
25. Deng, J., Cheng, L. and Wang, Z., 2020. Self-attention-based BiGRU and capsule network for named entity recognition. *arXiv preprint arXiv:2002.00735*.
26. He, G., Tian, J., Wang, X., Sun, L., Zhao, X. and Kexi, L., Time Series Variable Working Condition Co2 Corrosion Degree Prediction Model Embedded with Adabelief-Fuzzy Logic Algorithm Model. *Available at SSRN 5222783*.
27. https://data.mendeley.com/datasets/w5248v9fk3/1
28. Liu, Z., Zhang, Y. and Teng, G., 2025. Identification Method of Mature Wheat Varieties Based on Improved DenseNet Model. *Agriculture*, *15*(7), p.736.